TECHNICAL PAPER

CrossMark

Research of a non-linearity control algorithm for UAV target tracking based on fuzzy logic systems

Chaoying Pei[1] · Jingjuan Zhang[1] · Xueyun Wang[1] · Qian Zhang[1]

Abstract

Target tracking is one of the most widely used applications of UAVs and visual based tracking is the main method for non-cooperative tracking. In non-cooperative tracking missions, the UAV circles around the target and the gimbal rotates to keep the optic axis of the onboard camera pointing to the target. Compared with the biaxial gimbal, the single-axis gimbal system consists of only one torque motor, forming a great lightweight sensor suite, which also increases the requirement of the control accuracy. In the process of tracking moving target using a UAV with single-axis gimbal, there are still several challenges: (1) The completion of high precision and reliability of moving target tracking using UAV with only single-axis gimbal. (2) The non-linearity and uncertainty in the UAV system, where the non-linearity exists in the control of altitude, heading angle and roll angle. (3) The uncertainty in the expected turning radius of trajectory of the UAV when tracking a moving target without knowing its motion state. This paper proposes a vision-based fuzzy controller for a target tracking system consists of a fixed-wing UAV with single-axis gimbal. In this research, the innovations are described as follows: (1) A control algorithm is proposed for visual target tracking system consists of fixed-wing UAV with single-axis gimbal, which is able to guide the UAV to complete tracking task precisely and reliably. (2) Generation of roll command and heading command is immediately based on the information obtained from the images, skipping the step of calculating the velocity and position of the target, which can avoid unnecessary errors. (3) To deal with the non-linearities and uncertainties in the tracking system, seven fuzzy controllers are used to keep UAV circling around the target stably. (4) Flight tests are accomplished to verify the algorithm. Simulation results show that the maximum angle offset of the camera's optic axis is 0.04°, and the angle offsets can be kept in the range of 5° in the further flight test, which shows that the algorithm is able to accomplish the task of tracking a moving target successfully.

1 Introduction

Unmanned aerial vehicles (UAV) have been increasingly used in civil and military applications for dull, dirty and dangerous missions. Modern UAV applications include a wide variety of intelligence missions, such as search and rescue operations, area mapping, agricultural operation, etc. (Frew et al. 2008; Fu et al. 2012). With the development of both the photoelectric technology and UAV technology, combination of them has come into popularity and tracking UAVs attract more and more attention. These tracking UAVs implement missions such as surveillance, reconnaissance, rescue, counter-terrorism. The autonomous investigation and tracking of ground targets reflect the particular advantages for UAV in decreasing costs and great mobility.

Target tracking for UAV generally falls into two categories, cooperative tracking and non-cooperative tracking, respectively. In the cooperative tracking system, real-time between the UAV and the target is required, such as a convoy (Zhao 2014). Compared with cooperative tracking, non-cooperative tracking is with less limitation. Instead of real-time interaction, in the non-cooperative tracking system, the UAV is equipped with a gimbaled camera so that the information of the target can be obtained using vision-based method. For a successful tracking system, the target needs to be kept within the camera view and distinguished from the environment in real-time by the onboard computer. Then the visual information derived from the processing of images is used to control the rotation of the

✉ Xueyun Wang
  wangxueyun@gmail.com; succeedwade@sina.com

[1] School of Instrumentation Science and Opto-electronics Engineering, Beihang University, Beijing 100191, China

gimbal and the motion of UAV to track the target and keep it at the center of the image frame.

A series of researches related to this topic have been conducted recently. Part of them are related to cooperative tracking (Frew et al. 2008; Fu et al. 2012; Zhu et al. 2013; Oh et al. 2013). A method of cooperative tracking of a moving target by a team of unmanned aircraft based on a Lyapunov guidance vector field is proposed in Frew et al. (2008). A comprehensive ground target pursuit algorithm for fixed-wing UAV is proposed in Fu et al. (2012), in which the tracking algorithm is based on analysis and division of the possible path patterns. The simulation results demonstrate the stability and reliability of the algorithm. Papers Zhu et al. (2013) and Oh et al. (2013) proposes some innovative tracking and guidance methods, but these strategies are all analyzed in pure theoretical circumstances and verified only by simulation results. Dobrokhodov et al. (2008), Jabbari Asl and Do (2015), Asl and Bolandi (2014), Gomez-Balderas et al. (2013), Quintero et al. (2015) and Zhao and Chen (2015) proposes several methods for non-cooperative tracking of UAV. In Dobrokhodov et al. (2008), a UAV with a gimbaled camera and customized avionics is introduced. Although the proposed nonlinear control algorithm for integrated control for UAV and the gimbaled camera has obtained the predictive effect, the structure of pod has been complicated and a stabilized platform must be equipped for the camera. Jabbari Asl and Do (2015), Asl and Bolandi (2014) and Gomez-Balderas et al. (2013) proposes several methods for target tracking using quadrotors. Jabbari Asl and Do (2015) proposes an image-based visual servo (IBVS) controller for the 3D translational motion of the quadrotor UAV, using the flow of image features as the velocity information to compensate for the unreliable linear velocity data measured by accelerometers (Asl and Bolandi 2014). Nonlinear robust controllers are designed to deal with uncertainties in the dynamics of the image features and also uncertainties in the dynamics of the robot. Gomez-Balderas et al. (2013) proposes a control strategy consists of switching controllers, which allows making decisions when the target is lost temporarily or when it is out of the camera's field of view. However, compared with fixed-wing UAV, a quadrotor UAV is defective in its endurance and speed, which is always important for a tracking task. Quintero et al. (2015) proposes a method of using two UAVs to track an evasive vehicle, which ensures that one UAV is always close to the target at least. However, the use of two UAVs to track a target has increased the costs of the tracking task. Zhao and Chen (2015) proposes a method of calculating the position of target via Attitude and Heading Reference System (AHRS) and GNSS/Strapdown Inertial Navigation System (SINS) integrated navigation system, and visual system, but the calculating of the target position would import more errors, which can influence the accuracy and reliability of the tracking. For a fixed-wing UAV, the flight attitude and direction are manipulated by the deflection of the rudders and the mathematical models are complex with non-linearities and uncertainties, which can influence the accuracy and the reliability of the tracking task (Qadir et al. 2014; Dobrokhodov et al. 2006; Jurado et al. 2014). Beyond that, when tracking a moving target, the turn radius changes every time and there are also uncertainties in the calculation of the roll command which determines the turn radius in the flight.

In this research, the innovations are described as follows: (1) A control algorithm is proposed for visual target tracking system consists of fixed-wing UAV with single-axis gimbal, which is able to guide the UAV to complete tracking task precisely and reliably. (2) Generation of roll command and heading command is immediately based on the information obtained from the images, skipping the step of calculating the velocity and position of the target, which can avoid unnecessary errors. (3) To deal with the non-linearities and uncertainties in the tracking system, seven fuzzy controllers are used to keep UAV circling around the target stably. (4) Flight tests are accomplished to verify the algorithm.

The remaining part of the paper is organized as follows: in Sect. 2 the definition of coordinate systems, mathematical model and tracking framework are presented. Section 3 introduces tracking strategy and geometry between the UAV and target, and then the guidance algorithms is proposed to generate the command for both UAV turn-rate and single-axis system rotation. Numerical simulation, experimental results and actual flight test results are performed to verify the performances of the proposed methodology in Sect. 4. Finally, conclusion and future studies are provided in Sect. 5.

2 Overview of the tracking system

2.1 Coordinate definition of the UAV

The proposed UAV is shown in Fig. 1 The UAV is a V-empennage fixed-wing aircraft with a single-axis camera. To explain the tracking strategy in this paper clearly, the frames used in this paper are defined as follows.

The local geographical coordinate frame is called navigation frame (N-frame), the X_n-axis points to east in the local horizontal, Y_n-axis points to north in the local horizontal and Z_n-axis is defined according to the right-hand rule. The body coordinate frame (B-frame) is fixed to the UAV, X_b-axis points to the right of UAV, Y_b-axis points to the front and Z_b-axis is defined according to the right-hand rule. The camera coordinate frame (C-frame) is fixed to the
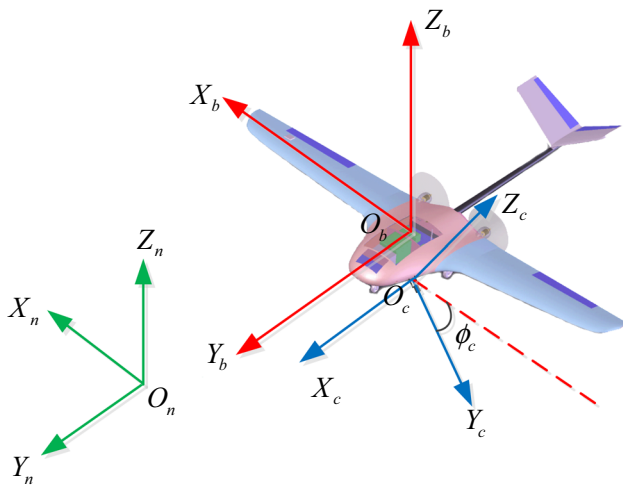
Fig. 1 The structure of UAV

(1)   Angular motion equations.

For this UAV, angular motion equations are as follows:

$$\begin{cases} \omega_x = \dot{\theta}\cos\gamma - \dot{\psi}\cos\theta\sin\phi \\ \omega_y = \dot{\phi} + \dot{\psi}\sin\theta \\ \omega_z = \dot{\theta}\sin\phi - \dot{\psi}\cos\theta\cos\phi \end{cases} \quad (2-3)$$

where θ, ϕ, ψ are the pitch, roll and heading angle of the UAV. ω_x, ω_y, ω_y are the projection of attitude angular acceleration on B-Frame.

(2)   Linear motion equations.

Linear motion equations can be expressed as follows:

$$\begin{cases} \dot{X} = V_x(\cos\psi\cos\gamma - \sin\psi\sin\theta\sin\gamma) - V_y\sin\psi\cos\theta + V_z(\cos\psi\sin\gamma + \sin\psi\sin\theta\cos\gamma) \\ \dot{Y} = V_x(\sin\psi\cos\gamma + \cos\psi\sin\theta\sin\gamma) + V_y\cos\psi\cos\theta + V_z(\sin\psi\sin\gamma - \cos\psi\sin\theta\cos\gamma) \\ \dot{Z} = -V_x\cos\theta\sin\gamma + V_y\sin\theta + V_z\cos\theta\cos\gamma \end{cases} \quad (2-4)$$

camera, Y_c-axis is defined according to the optical axis, X_c-axis is the rotation axis of camera, which is aligned with Y_b-axis. Z_c-axis is defined according to the right-hand rule. The image coordinate frame (I-frame) is fixed to the image, Y_i-axis and X_i-axis are parallel to the X_c and Y_c. The camera could only be rotated around the X_c-axis and the pitch angle of Y_c-axis is defined as γ_c.

2.2 Mathematical model of the UAV

In this paper, we use a 6-DOF UAV, and here we choose geographic coordinates (N-frame) as static coordinate and body coordinate frame (B-frame) as moving coordinate. Under the action of external resultant force $\vec{F}$, the linear dynamic equation can be expressed as:

$$\frac{\vec{F}}{m} = \frac{d\vec{V}}{dt} + \vec{\omega} \times \vec{V} \quad (2-1)$$

where $\vec{V}$ is the velocity of the UAV, $\vec{\omega}$ is the angular velocity of the UAV, m is the mass of the UAV.

Under the action of external resultant moment $\vec{M}$, the angular momentum can be expressed as:

$$\vec{M} = \frac{d\vec{H}}{dt} + \vec{\omega} \times \vec{H} \quad (2-2)$$

where $\vec{H}$ is the moment of momentum.

V_x, V_y, V_z are projections of velocity on B-Frame, and $\dot{X}$, $\dot{Y}$, $\dot{Z}$ are projections of velocity on N-Frame.

2.3 Control mechanisms of the UAV

In this UAV system, there are five control mechanisms: elevator, rudder, aileron, throttle and camera gimbal. By controlling the mechanisms, the force and moment acting on the UAV as well as the direction of the camera's optical axis get changed, thus controlling the UAV to track the target. The parameters of the mechanisms are defined as follows:

Deflection angle of the elevator ΔU_θ: For elevator, upward direction is positive.

Deflection angle of the rudder ΔU_ψ: For rudder, deflection to the left is positive.

Deflection angle of the ailerons ΔU_ϕ: For left aileron, upward deflection is positive, while for right aileron, downward deflection is positive.

Tension of the engine (throttle) δ_T: In this UAV system, throttle is controlled by propeller speed, and the increase of the speed is taken as positive.

Deflection angle of the camera gimbal ΔU_{ϕ_c}: For camera gimbal, upward direction is positive.
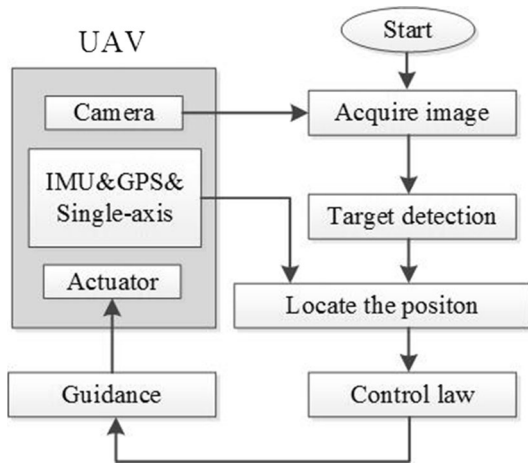
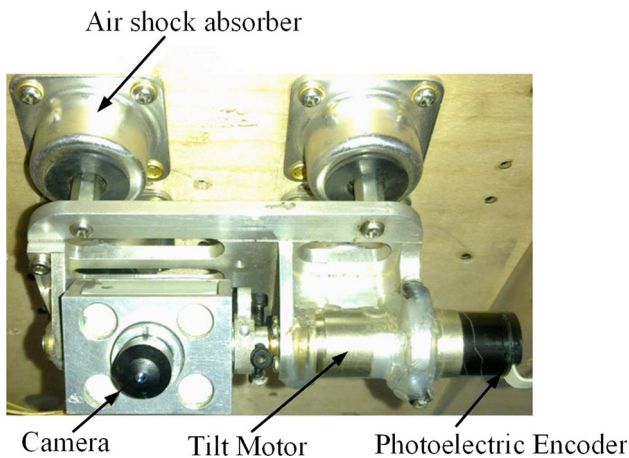Fig. 2 The flowchart of the tracking strategy

Fig. 3 single-axis vision system

2.4 Autonomous tracking framework

The flowchart of the proposed framework is shown in Fig. 2. The system architecture can be described in brief as acquire image, target detection, calculates the position error between image center and target, estimates the control instruction of UAV and single-axis camera.

The image is acquired by a single-axis vision system that is shown in Fig. 3. The vision system is mounted by four air shock absorbers on the aircraft for isolating the vibration. A torque motor is used to drive the camera rotating around the pitch axis and photoelectric encoder is equipped for angle feedback.

For detecting the target from the raw image of the camera, the image is transformed into a grey scale image and a Laplacian operator is performed on it to sharpen the difference between the target and surroundings. Then, an adaptive threshold is used to isolate the target from the input image. The algorithm of the image extraction has been used in many articles (Wang et al. 2014; Jurado et al.
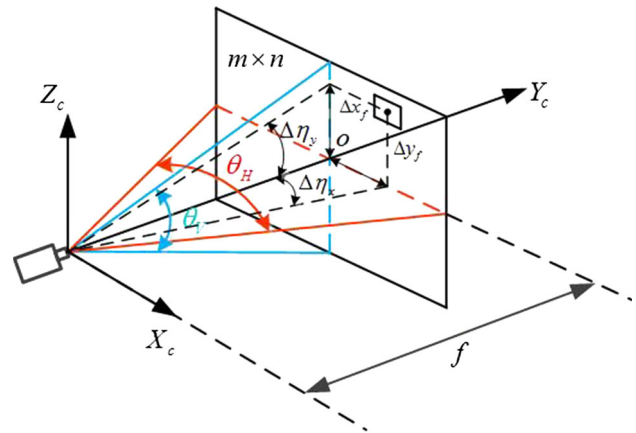

Fig. 4 The relationship of angle offsets and deviations in image

2014; Mao and Jain 1999; Starner et al. 2003; Clausi and Zhao 2003; Shan et al. 2007), the detail description has been omitted here. However, considering the occasional misidentification occurs, the ground operators could re-select the target at the control station.

After the target being detected in the image, the offsets between target and collimation axis can be determined by calculating the pixel points. The angle offsets are described briefly in Fig. 4. The resolution of camera is $m \times n$ and focal length is f, the side length of pixel point is s, then the viewing angle of horizontal and vertical can be calculated in Eq. 2-5 and the angle offsets can be calculated in Eq. 2-6.

$$\theta_H = 2\tan^{-1}\left(\frac{m \cdot s}{2f}\right), \ \theta_V = 2\tan^{-1}\left(\frac{n \cdot s}{2f}\right) \quad (2-5)$$

$$\Delta\eta_x = arc\tan\left(\frac{\Delta x_f}{f}\right), \ \Delta\eta_y = arc\tan\left(\frac{\Delta y_f}{f}\right). \quad (2-6)$$

As the camera is equipped under the abdomen of UAV, the X angle offset $\Delta\eta_x$ can be regarded as control error of azimuth angle and Y angle offset $\Delta\eta_y$ can be regarded as control error of single-axis vision system. In this paper, the relative position of UAV to target is the fixed altitude and circle radius; therefore, the offsets can be used as feedback for control system.

3 Control system development

3.1 Tracking strategy

Figure 5 illustrates the geometry between the UAV and target. As shown in Fig. 5, define the position of the target as the origin point O_n, and R is the circle radius and H is the circle altitude. At this time, the relative inclination angle of UAV to target is ρ and the angular deviation between
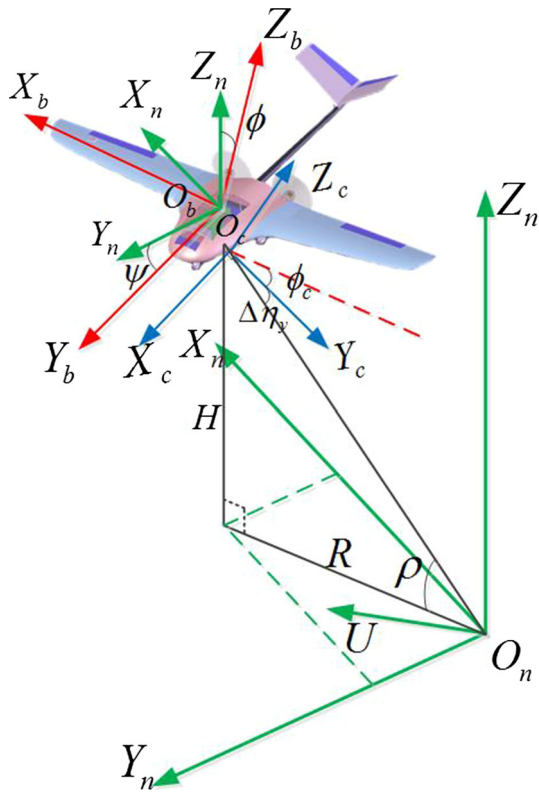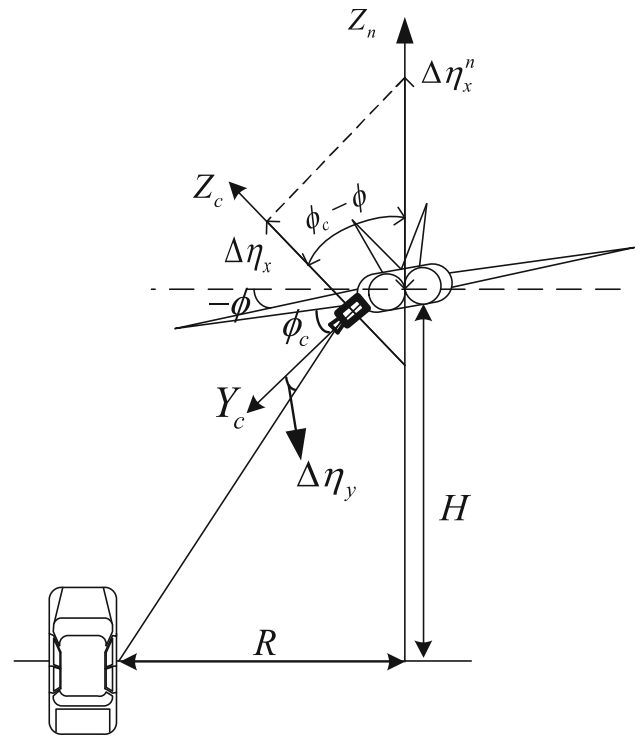
Fig. 5 Geometry between UAV and target
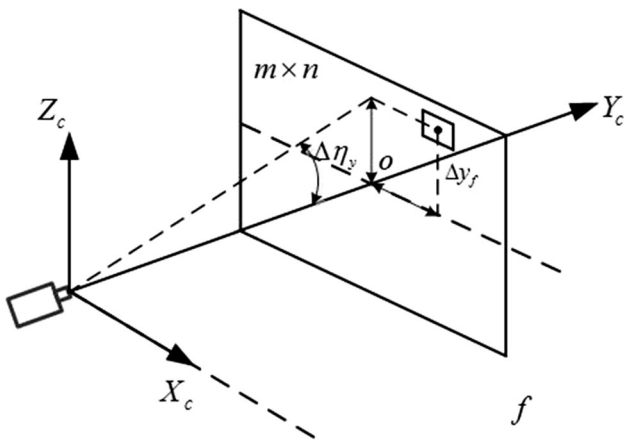

Fig. 7 Sketch of the offsets angle

Fig. 6 Elimination of the offset Δy_f

Fig. 8 Change of offsets caused by rotation around optical axis

optical axis and target is $\Delta \eta_y$. Therefore, the single-axis vision system should be controlled to eliminate the vertical offset. As the velocity vector is U, the azimuth angle should be controlled in order to make sure that the relative velocity in $O_c Y_c$ is zero.

To eliminate the offset in the obtained image, the camera should be rotated around X_c and Z_c as is shown in the Fig. 6. Rotation around X_c can be implemented by adjusting the camera gimbal, as is shown in the Fig. 6. By
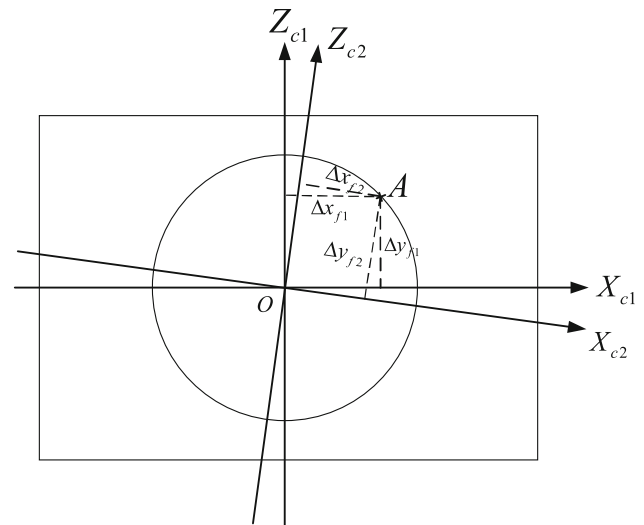
rotating the camera around X_c, the offset Δy_f can be eliminated.

The elimination of Δx_f is implemented by controlling the heading angle of the UAV which is on the Zn axis. However, to eliminate the offset Δx_f, the camera is expected to turn an angle $\Delta \eta_x$ around Z_c axis. As is shown in the Fig. 7, Zn axis is inconsistent with Z_c axis. The rotation on the Zn axis can be decomposed to Z_c axis and Y_c axis. The component on the Z_c should be $\Delta \eta_x$. According to
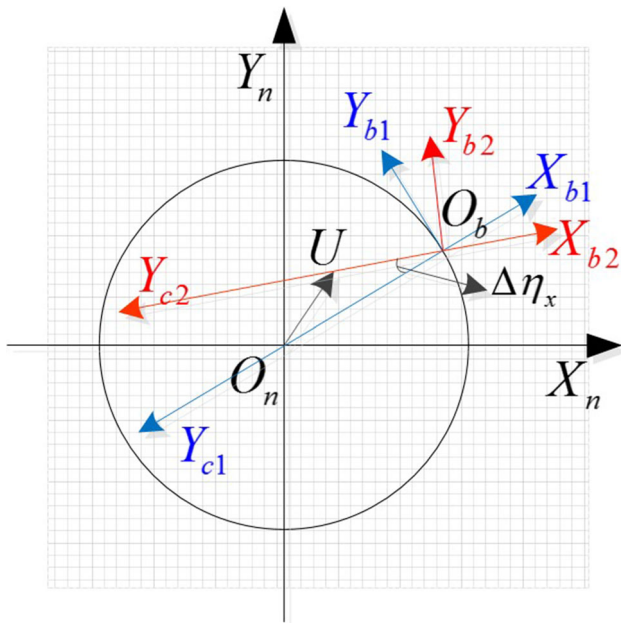
Fig. 9 Horizontal projection of the tracking strategy

the relationship between Z_c and Z_n, $\Delta\eta_x^n$ can be expressed as follow:

$$\Delta\eta_x^n = \frac{\Delta\eta_x}{\cos(\phi_c - \phi)}. \qquad (3-1)$$

From the Fig. 7, we can see that the rotation around Z_n can also cause the rotation around Y_c. As is shown in the Fig. 8, when the camera coordinate system rotates around Y_c (from $X_{c1}Y_{c1}Z_{c1}$ to $X_{c2}Y_{c2}Z_{c2}$), the offsets Δx_{f1} and Δy_{f1} will change to Δx_{f2} and Δy_{f2}. However, as Y_c is collinear with the optical axis of camera, the rotation around it will not cause increment of distance between the target and the center of the image, so that by controlling two visual variables the offset between target and the center of the image can be eliminated effectively.

Considering Fig. 9, illustrate the horizontal projection of the tracking strategy. Due to the movement of target, the

coordinate frame of UAV is translated from $O_bX_{b1}Y_{b1}$ to $O_bX_{b2}Y_{b2}$ and the angular deviation is $\Delta\eta_x$. Then, the azimuth angle of UAV should be adjusted to make the optical axis coincide with the target.

When tracking a stationary target, the UAV is expected to hover along a circular trajectory centered in the target, maintaining a fixed radius. In such a situation, the roll angle is fixed and can be calculated as:

$$\phi = a\tan\left(\frac{v^2}{R \times g}\right) \qquad (3-2)$$

where ϕ is roll angle of the UAV, v is the horizontal velocity of the UAV, R is the expected radius, g is acceleration of gravity.

In most cases, motion of the target is not negligible. When tracking a moving target, the curvature of the expected trajectory changes with the movement of the target. As is shown in the Fig. 10, as the target skip from point p1 to point p11 (via p2–p10), the curvature of the trajectory changes among R1, R2, R3. However, it can be conceivable that, continuous movement of the target will cause changes of the expected turning radius of the UAV. In the UAV system, the curvature of the trajectory is mainly controlled by the roll angle of the UAV. Considering this, the instruction of the roll angle and the azimuth angle should be in coordination based on the angular deviation $\Delta\eta_x$.

3.2 Guidance and control law

In this section, the guiding method for UAV is described. As the UAV studied in this paper is a normal fixed-wing aircraft, the three attitude channels of the UAV are decoupled and could be controlled separately. To track successfully, the target needs to be kept within the camera view. When the camera is mounted on the UAV with a single-axis, the visual information derived from the images is used to control the motion of the UAV and the camera. However, in most cases, the relative velocity the target is
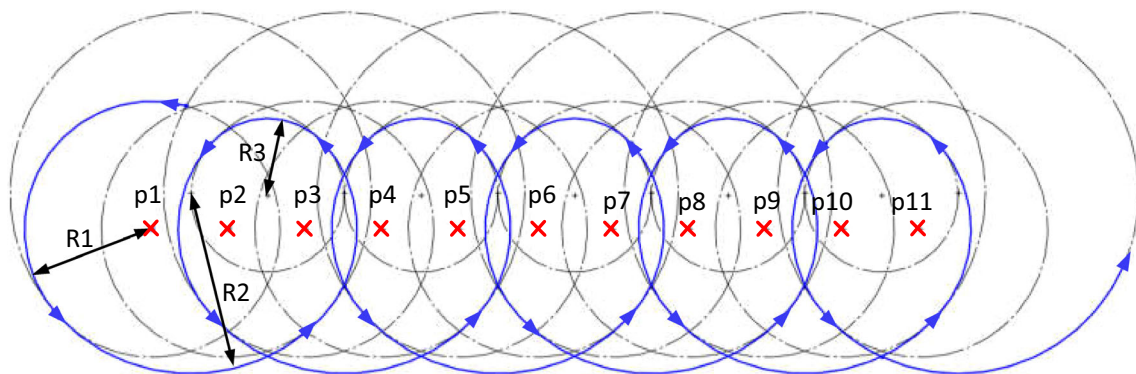

Fig. 10 The change of curvature of trajectory
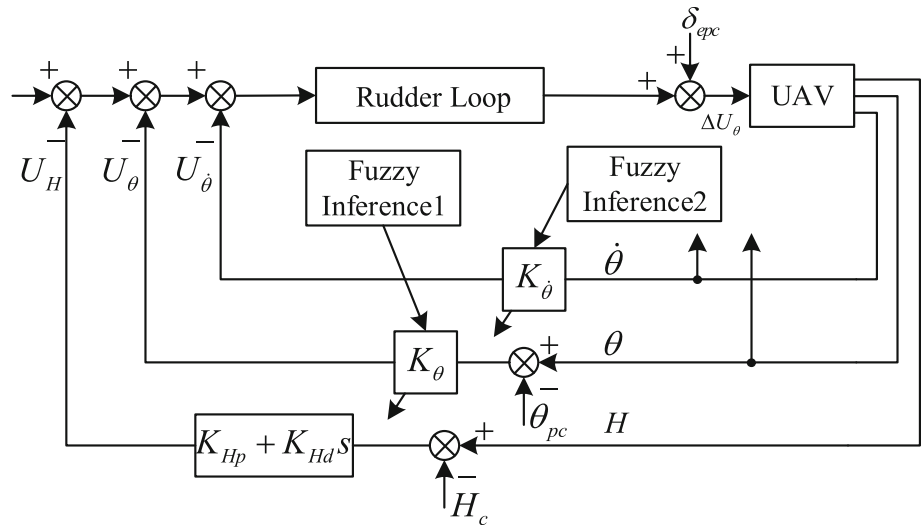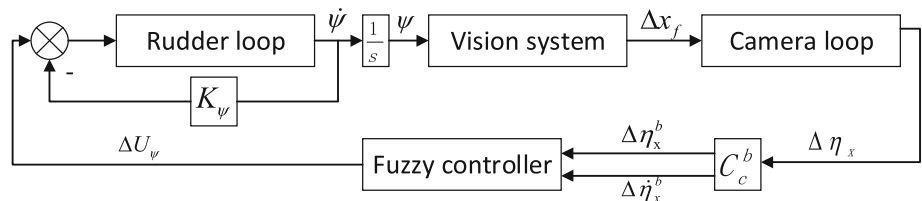
Fig. 11 Controller for pitch channel

Fig. 12 Controller for heading channel

negligible, meanwhile, the uncertainty and disturbance of the system should be taken into consideration. To deal with problems above, in this paper, we proposed a fuzzy control algorithm for the three axes UAV movement and the single-axis camera movement. Fuzzy logic control has been widely researched for the last decade, and it has been implemented on various dynamical systems (Zhang et al. 2017; Shen et al. 2017; Jin et al. 2017).

For pitch channel, the deflection angle of elevator causes the changes of pitch angle and altitude. Figure 11 indicates the pitch channel control method with three feedback loops.

In the controller, δ_{epc} and θ_{pc} are all values for initial trim. In order to improve the robustness of the attitude, a fuzzy logic controller is introduced to compensate the coefficients uncertainty. Here, the pitch angle θ and

deviation $\dot{\theta}$ are regarded as the inputs of the two fuzzy controllers and control law coefficient error is the output.

For heading channel, the deflection between the ideal direction and the actual direction of the optical axis causes the target's deviation to midpoint in the obtained image. As is shown in the Fig. 12, $\Delta\eta_y$, the horizontal deviation in the image can be eliminated by adjusting the heading angle of UAV. In heading channel, the heading angle is mainly controlled by the rudder. Thus, for the heading channel, the horizontal deviation $\Delta\eta_x$ and its derivative $\Delta\dot{\eta}_x$ are the inputs of the system model, with control variable of rudder as output. However, transfer function of the system model is nonlinear and affected by several factors, such as the attitude of UAV, wind velocity, the relative position and the velocity of the target and UAV, as well as uncertain disturbances. Considering all above, here we use a fuzzy

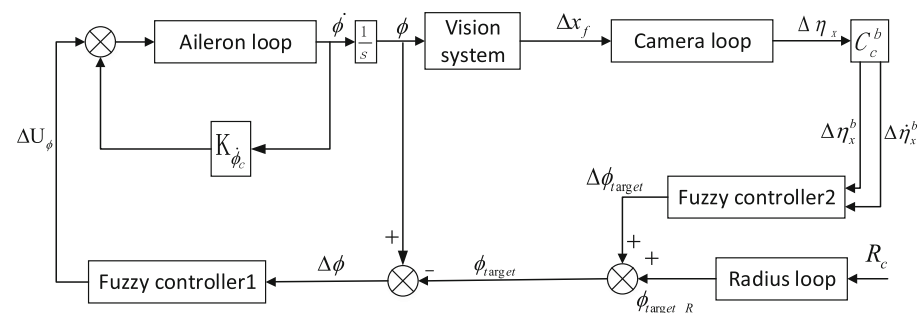**Fig. 13** Controller for roll channel
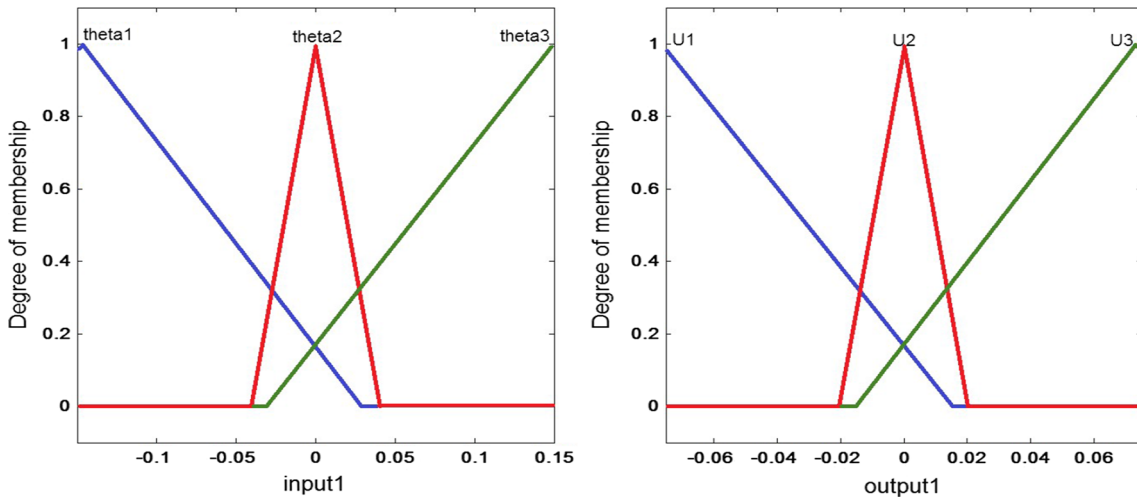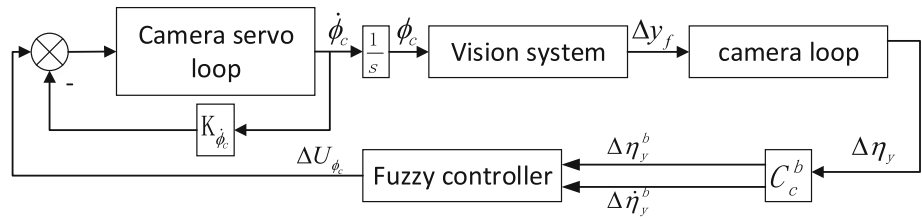
Fig. 14 Controller for gimbal channel

Fig. 15 Membership function of $\Delta\theta$ (input) and ΔU_θ (output)

Table 1 Rules of fuzzy controller 1 in pitch channel

Input	Output
Theta1	U1
Theta2	U2
Theta3	U3

controller to generate rudder commands with $\Delta\eta_x$ and $\Delta\dot{\eta}_x$ as inputs, as is indicated in the Fig. 12.

In the controller, ψ is the heading angle of UAV, Δx_f is the target's horizontal deviation in the obtained image, $\Delta\eta_x$ is the angle offset of the optical axis, ΔU_ψ is the rudder command generated by Fuzzy controller, $\Delta\eta_x^b$ is the projection of $\Delta\eta_x$ on the body coordinate frame (B-frame), $\Delta\dot{\eta}_x^b$ is the increment of $\Delta\eta_x^b$, which is calculated by:

$$\Delta\dot{\eta}_{x(i)}^n = \frac{\Delta\eta_{x(i)}^n - \Delta\eta_{x(i-1)}^n}{\mathrm{Dt}}. \tag{3-3}$$

As is discussed in Fig. 10, the command of the roll channel should be coordinate with the movement of the target, controlling UAV to track and hover around it. In the case that the target is moving far away from the UAV, to track successfully, the turning radius is expected to

increase. When the target stops moving, UAV start hovering with fixed roll angle computed by the fixed radius. Therefore, in the controller, the reference value of the target roll angle depends on the appointed turning radius of the UAV in the case of tracking a stationary target. When the targets move, the position of the target in the image changes, and the camera loop will output the horizontal deviation $\Delta\eta_x^b$. The first fuzzy controller is then constructed, with $\Delta\eta_x^b$ and $\Delta\dot{\eta}_x^b$ as inputs, and deviation of target roll angle $\Delta\phi_{\mathrm{target}}$ as output. The output of the controller, $\Delta\phi_{\mathrm{target}}$, is used to adjust the target roll angle so that the UAV can track the moving target, while $\Delta\phi_{\mathrm{target\_R}}$, the reference value of the target roll angle is used to maintain the radius of the steady state of the trajectory radius.

The second fuzzy controller in roll channel is used to ensure the roll angle in reality to keep up with the computed target roll angle. The inputs of the second fuzzy controller are the difference between actual roll angle and target roll angle $\Delta\phi$ and its derivative $\Delta\dot{\phi}$, and the output is control variable of the aileron of the UAV. The roll channel controller is shown in the Fig. 13.

Table 2 Parameters of fuzzy controller 1 in pitch channel

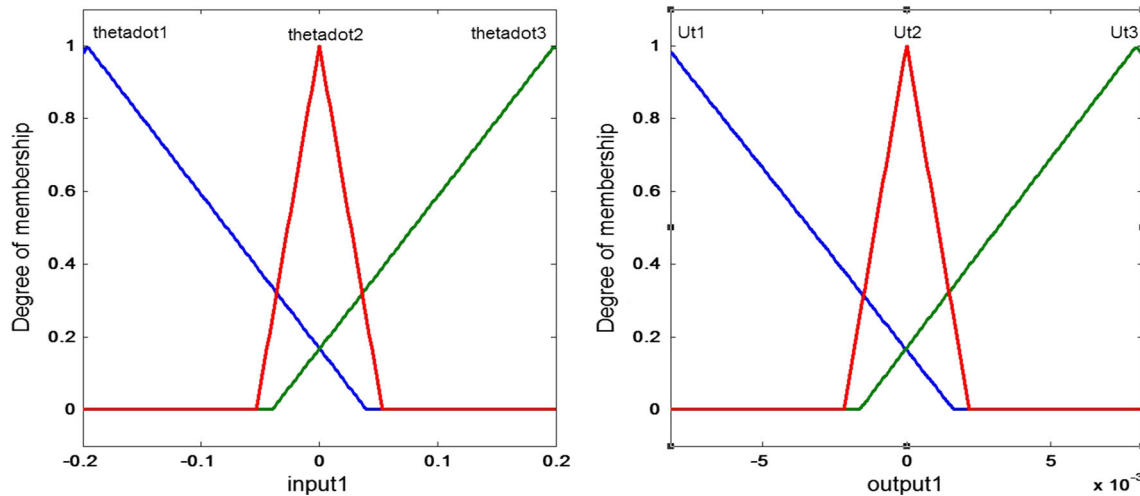| And method	Or method	Implication	Aggregation	Defuzzification
Min	Max	Min	Max	Centroid

Fig. 16 Membership function of $\Delta\dot{\theta}$ (input) and ΔU_θ (output)

Table 3 Rules of fuzzy controller 2 in pitch channel

Input	Output
Thetadot1	U1
Thetadot2	U2
Thetadot3	U3

Table 4 Parameters of fuzzy controller 2 in pitch channel

And method	Or method	Implication	Aggregation	Defuzzification
Min	Max	Min	Max	Centroid

In the flowchart above, $\dot{\phi}$ is the roll angular velocity obtained by sensors on the UAV, and can be integrated to compute roll angle ϕ. $\phi_{\text{target\_R}}$ is the reference value of target roll angle computed by an appointed hover radius. $\Delta\phi_{\text{target}}$ is the increment value of target roll angle computed by the first Fuzzy controller. ϕ_{target} is target roll angle. $\Delta\phi$ is the difference between target roll angle and actual roll angle. ΔU_ϕ is control variable of the aileron of the UAV.

The camera gimbal drives the camera to rotate around X_c-axis and the rotation of the camera can eliminate the vertical deviation Δy_f, as is shown in the Fig. 14. Similar to the controller of heading channel, the inputs of the Fuzzy controller here are $\Delta\eta_y^b$ and $\Delta\dot{\eta}_y^b$, and the output of it is the control variable of the gimbal ΔU_{ϕ_c}.

In the controller, ϕ_c is the pitch angle of the camera, Δy_f is the target's vertical deviation in the obtained image, $\Delta\eta_y$ is the angle offset of the optical axis, ΔU_{ϕ_c} is the gimbal command generated by Fuzzy controller, $\Delta\eta_y^b$ is the projection of $\Delta\eta_y$ on the body coordinate frame (B-frame), $\Delta\dot{\eta}_y^b$ is the increment of $\Delta\eta_y^b$, which is calculated by:

$$\Delta\dot{\eta}_{y(i)}^n = \frac{\Delta\eta_{y(i)}^n - \Delta\eta_{y(i-1)}^n}{Dt}. \qquad (3-3)$$

4 Simulation and experimental results

4.1 Simulation results

4.1.1 Pitch channel

4.1.1.1 Fuzzy controller1 Parameters of fuzzy controllers are set from experience. The following figures shows the Membership functions of the fuzzy controller1 for pitch channel (Fig. 15).

Tables 1 and 2 shows the rules and other parameters of the fuzzy logic control of Fuzzy controller1 in the pitch channel.

4.1.1.2 Fuzzy controller2 The following figures shows the Membership functions of the fuzzy controller2 for pitch channel (Fig. 16).

Tables 3 and 4 shows the rules and other parameters of the fuzzy logic control of Fuzzy controller2 in the pitch channel.

4.1.2 Heading channel

The following figures shows the Membership functions of the fuzzy controller for heading channel (Fig. 17).

Tables 5 and 6 shows the rules and other parameters of the fuzzy logic control of Fuzzy controller in the heading channel.
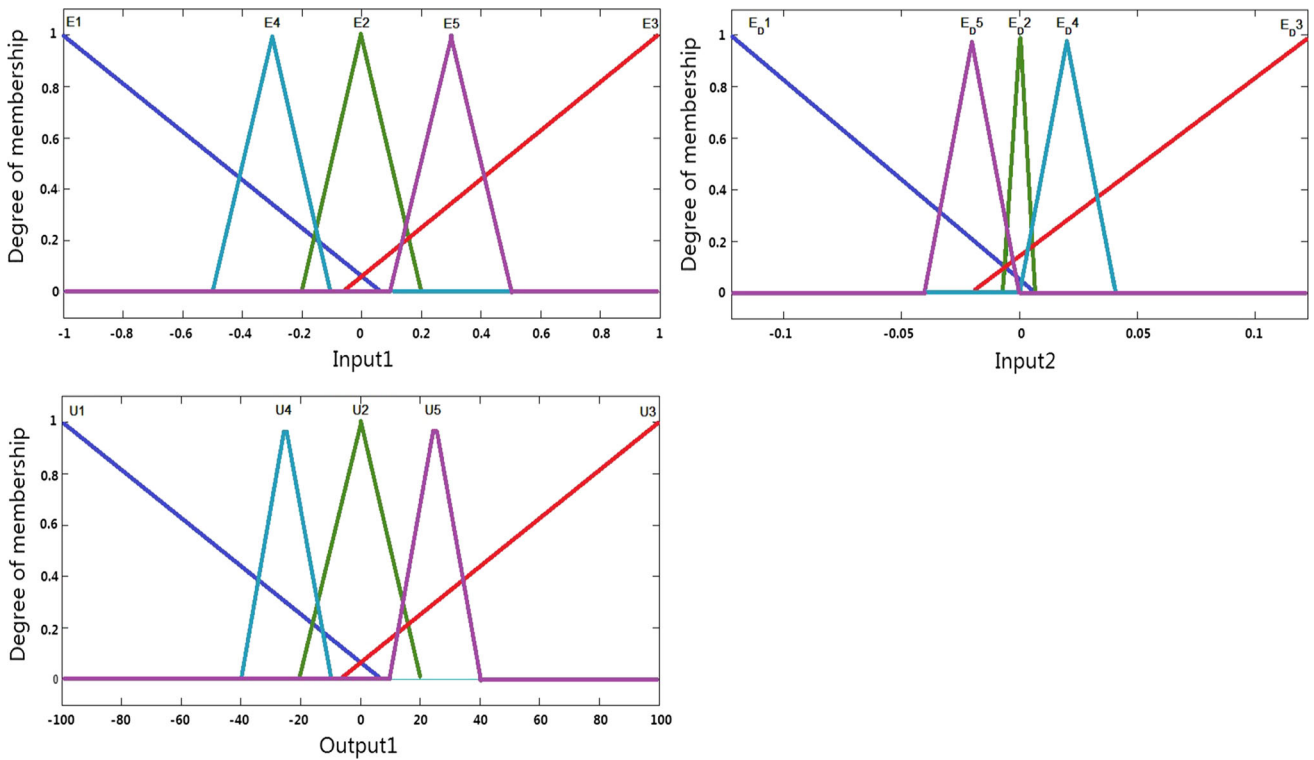
Fig. 17 Membership function $\Delta\eta_{Ix}^b$ (input1), $\Delta\dot{\eta}_x^b$ (input2) and ΔU_ψ (output)

Table 5 Rules of fuzzy controller in heading channel

	E1	E2	E3	E4	E5
E_DOT1	U1	U1	U2	U1	U2
E_DOT2	U2	U2	U3	U2	U4
E_DOT3	U2	U2	U3	U2	U5
E_DOT4	U2	U5	U5	U4	U5
E_DOT5	U4	U2	U5	U4	U5

Table 6 Parameters of fuzzy controller in heading channel

And method	Or method	Implication	Aggregation	Defuzzification
Min	Max	Min	Max	Centroid

4.1.3 Roll channel

4.1.3.1 Fuzzy controller1 In the roll channel, there are two fuzzy controllers. The following figures show the
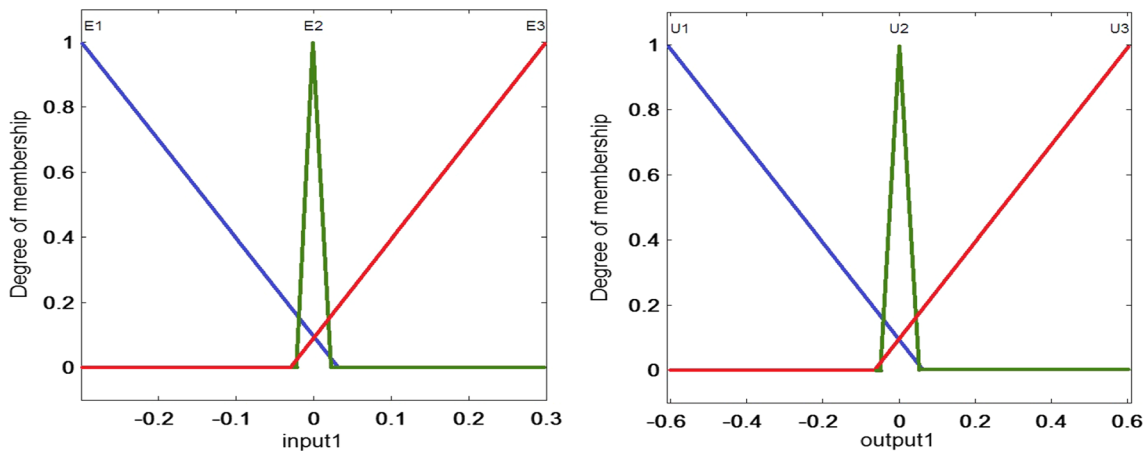

Fig. 18 Membership function of $\Delta\phi$ (input) and ΔU_ϕ (output)

Table 7 Rules of fuzzy controller1 in roll channel

Input	Output
E1	U1
E2	U2
E3	U3

Table 8 Parameters of fuzzy controller 1 in roll channel

And method	Or method	Implication	Aggregation	Defuzzification
Min	Max	Min	Max	Centroid

Membership function of fuzzy controller1 in roll channel with single input and single output (Fig. 18).

Tables 7 and 8 shows the rules and other parameters of the fuzzy logic control of Fuzzy controller 1 in the roll channel.

4.1.3.2 Fuzzy controller2 The following figures show the Membership function of fuzzy controller2 in roll channel with two inputs and single output (Fig. 19).

Table 9 Rules of fuzzy controller 2 in roll channel

	E1	E2	E3
E_D1	U3	U2	U2
E_D2	U2	U2	U2
E_D3	U2	U2	U1

Table 10 Parameters of fuzzy controller 2 in roll channel

And method	Or method	Implication	Aggregation	Defuzzification
Min	Max	Min	Max	Centroid

Tables 9 and 10 shows the rules and other parameters of the fuzzy logic control of Fuzzy controller 2 in the roll channel.

4.1.4 Controller for camera gimbal

The following figures show the Membership function of fuzzy controller for camera gimbal with two inputs and single output (Fig. 20).
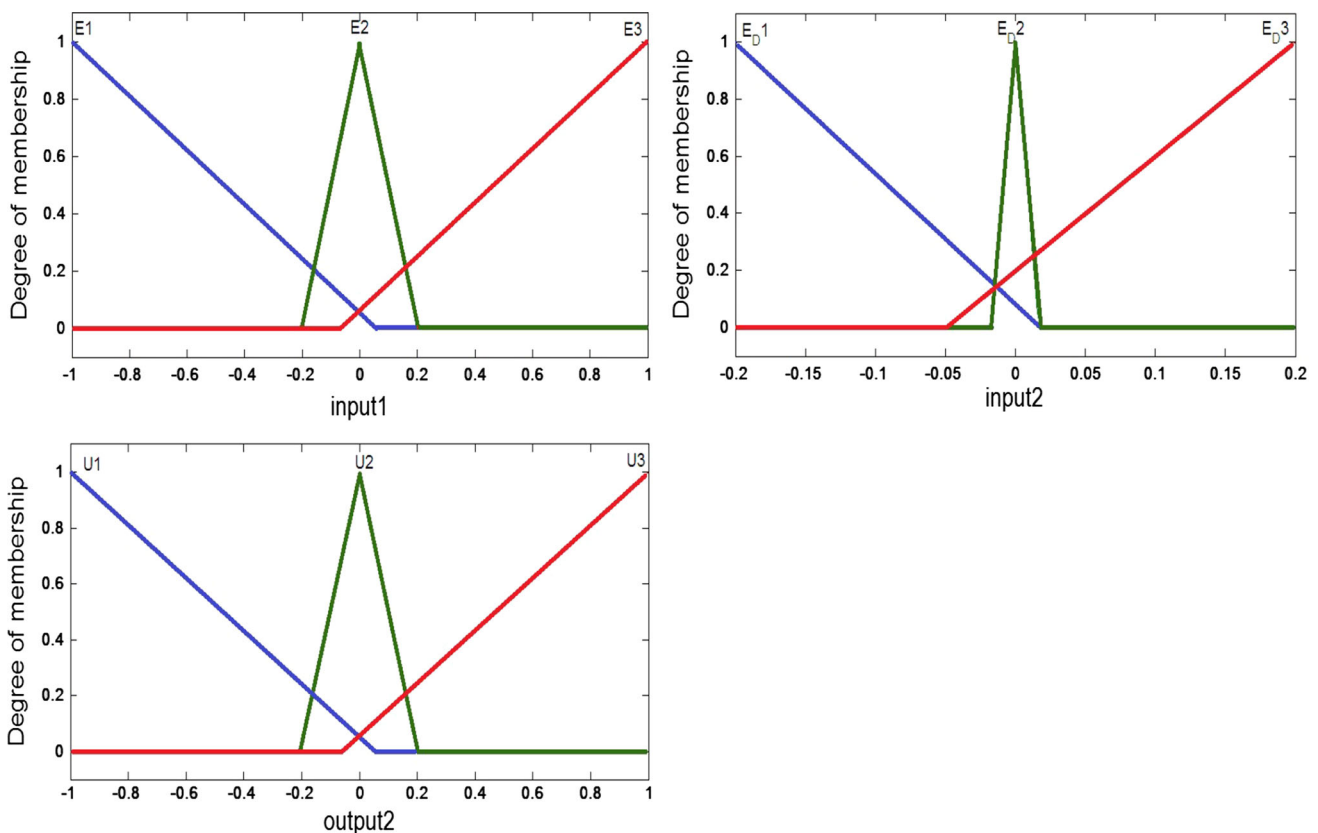

Fig. 19 Membership function of $\Delta\eta_x^b$ (input1), $\Delta\dot{\eta}_x^b$ (input2) and $\Delta\phi_{\text{target}}$ (output)
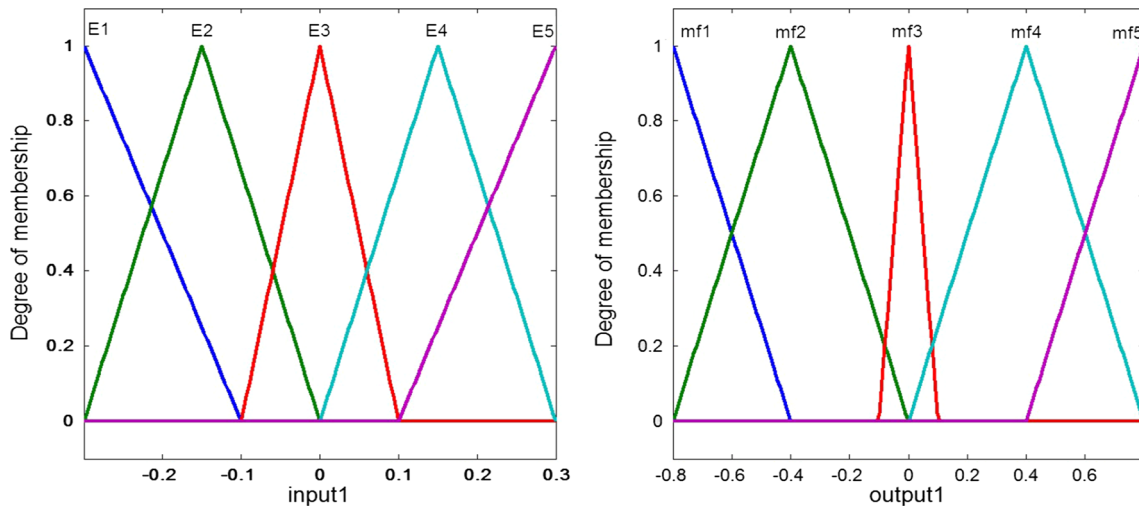
Fig. 20 Membership function of $\Delta\eta_y^b$ (input) and $\Delta\dot{\eta}_y^b$ (output)

Table 11 Rules of fuzzy controller in gimbal channel

	E1	E2	E3	E4	E5
E_D1	U1	U2	U3	U3	U3
E_D2	U2	U2	U3	U3	U3
E_D3	U2	U2	U3	U3	U4
E_D4	U2	U2	U3	U4	U5
E_D5	U2	U3	U3	U4	U5

Table 12 Parameters of fuzzy controller in gimbal channel

And method	Or method	Implication	Aggregation	Defuzzification
Min	Max	Min	Max	Centroid

Tables 11 and 12 shows the rules and other parameters of the fuzzy logic control of Fuzzy controller for camera gimbal.

4.1.5 Simulation results

To verify the effects of the fuzzy controllers, the target in the simulation moves in sine wave track, and its velocity are expressed as follows:

$$\begin{cases} v_x = 2.5 \text{ m/s} \\ v_y = 10\sin(0.001x) \end{cases}$$

v_x is the velocity on the X_n-axis, v_y is the velocity on the Y_n-axis, x is the UAV's displacement on X_n-axis.
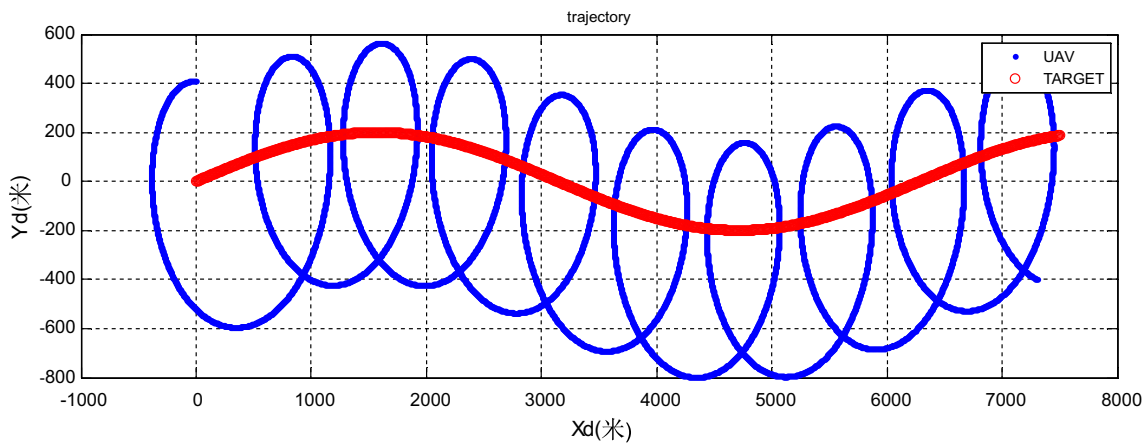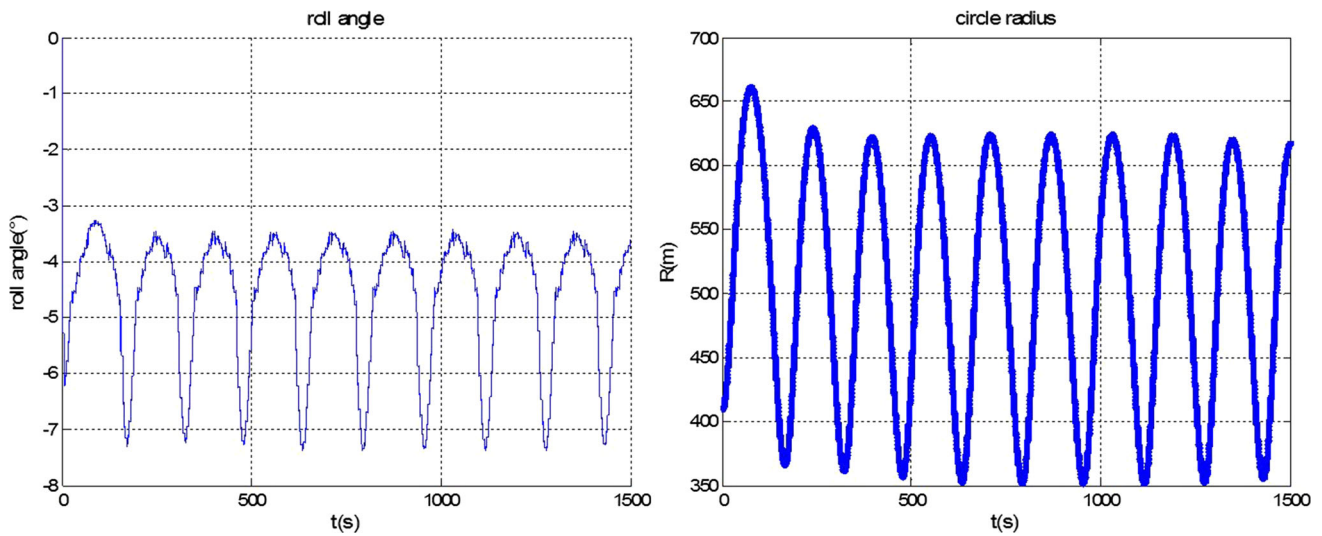

Fig. 21 Trajectory of simulation result

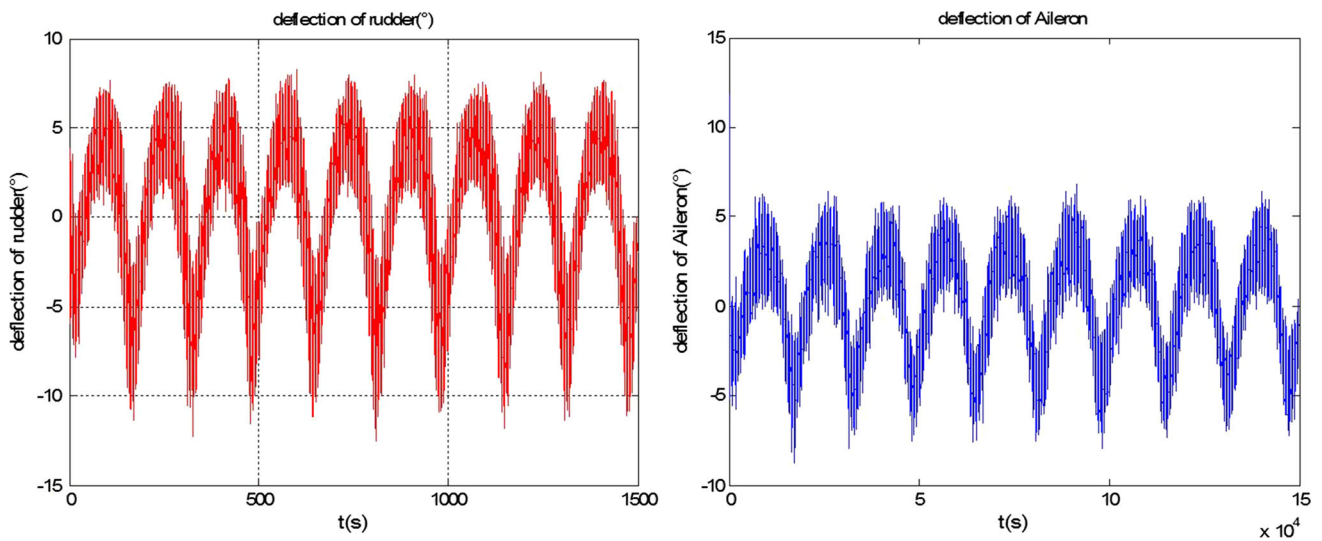**Fig. 22** Roll angle and circle radius of UAV in simulation result

Fig. 23 Deflection of aileron and rudder

When tracking, the system detects the deviation of the target from the center of the image and generates roll and heading command for the circling of the UAV, and the rotation command for the camera around the single axis. Meanwhile, the pitch channel is controlled by the fuzzy controllers to keep UAV flying at a constant height. Here we set the command of flight altitude as 200 m, and the hover radius as 500 m (Figs. 21, 22). The simulation results are as follows:

Above figure shows the simulation results of the tracking. When the target moves in sine wave track, UAV circles around the target with the optic axis of the camera pointing to the target (Fig. 23).

Figure above shows as the target moves, the roll angle of UAV changes and circle radius changes around the radius command (500 m) (Figs. 24, 25).

The figures above show the deviation angles in X_c and Y_c axis. When the UAV starts hovering around the target, the deviation angle in Y_c axis is within the range of $(-0.005° \sim 0.005°)$ and the deviation angle in X_c is within the range of $(-0.04 \sim 0.02)$. Considering the focal length of the camera is 35 mm, the deviation distance in the Y axis of the image is within the range of $(-0.175 \sim 0.175$ mm), and the deviation distance in the X axis of the image is within the range of $(-1.4 \sim 0.7$ mm) (Fig. 26).
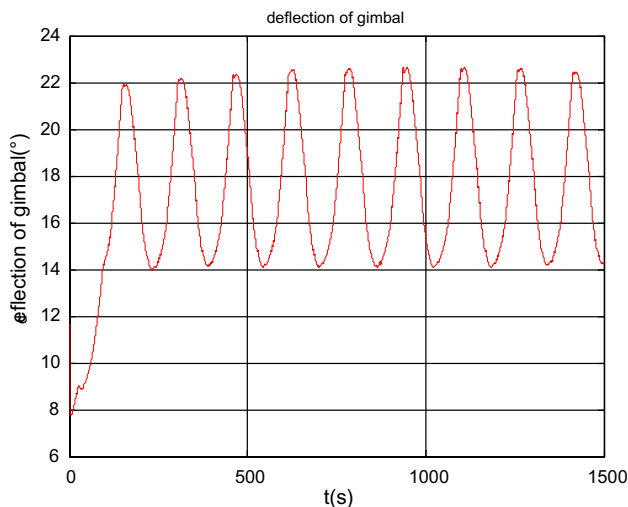
Fig. 24 Deflection of gimbal

Fig. 26 Trajectory with fixed roll command

The above figure shows the results of tracking with fixed roll command instead of changing roll commands with the motion of target. The figure shows the UAV can hover around the target at first, but fail to track it as the target moves.

4.2 Flight test

Actual flight tests were conducted to verify the controller algorithm. The flight tests validate the algorithm and shows that the tracking system is capable of generating accurate roll and heading command for the UAV and the angle position command for the single-axis gimbal, keeping the target at the center of the image frame. The UAV was
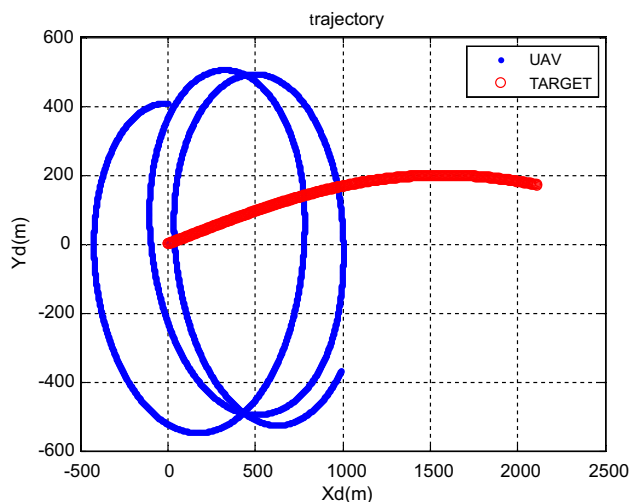
flying at the altitude of 200 m and the circle radius is chosen to be 500 m and the trajectory. The video captured by the camera, as is shown in the Fig. 27, was broadcast to the ground computer, and the target was a running car. Once the UAV detected the target, it started circling around it and tracking its motion. The gimbal also rotated as the relative position of UAV and target changed. In the Flight test, the deviation angle of the target in the X_c was within the range of $(-5° \sim 5°)$, and the deviation angle in the Y_c was within the range of $(-3° \sim 3°)$. The results of the flight test show that the control algorithm based on fuzzy logics can provide the UAV the ability of tracking moving targets (Fig. 28).
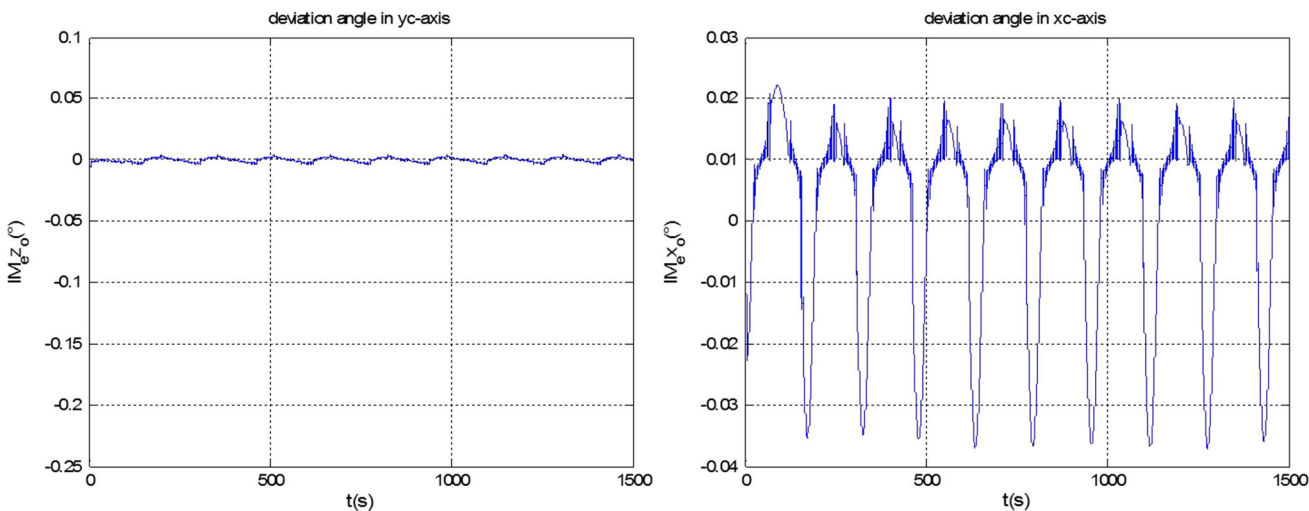

Fig. 25 Deviation angle in simulation results
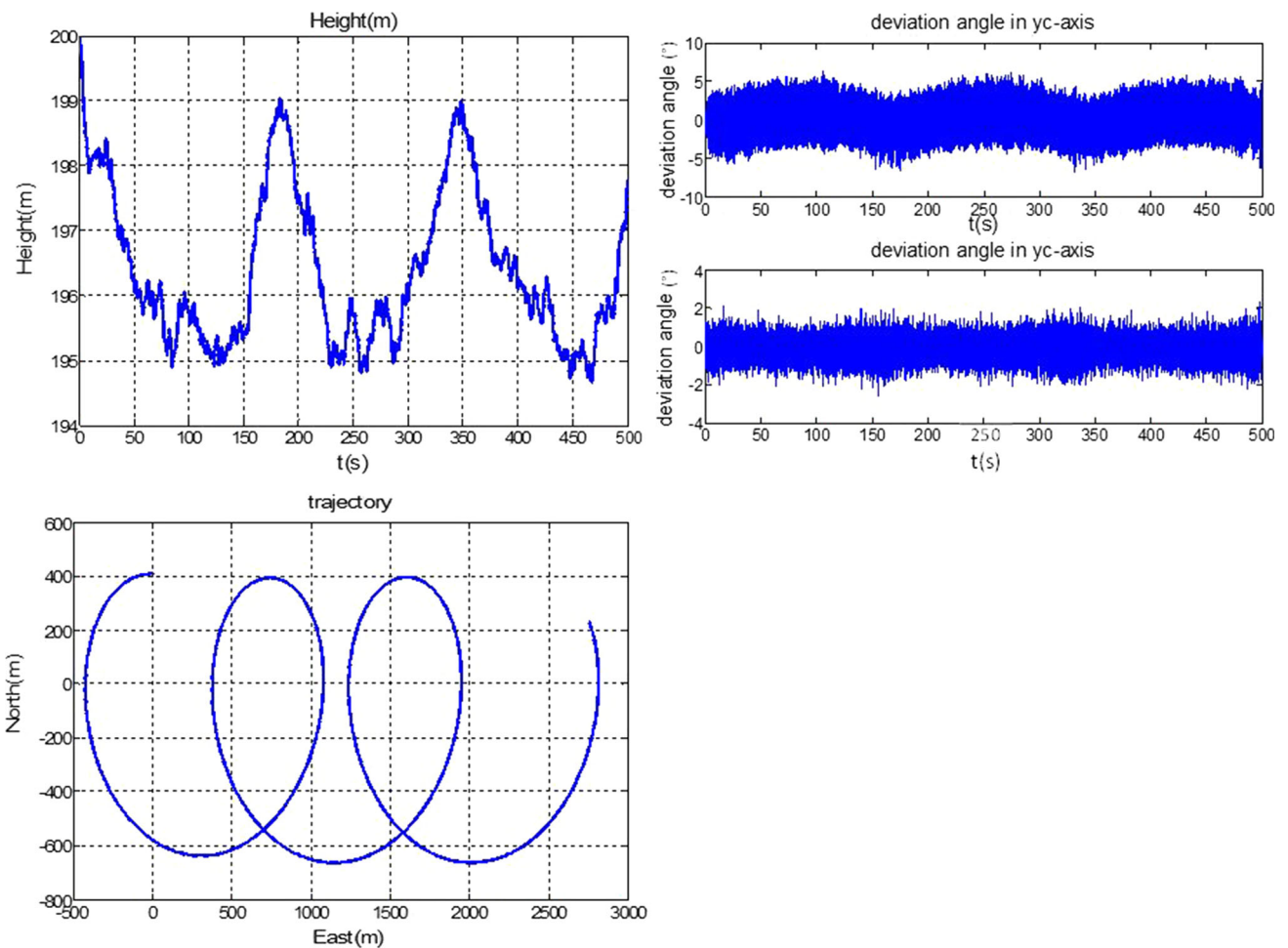
Fig. 27 Pictures taken in flight test

Fig. 28 Results of actual flight test

5 Conclusion

In this paper, an innovative vision based target tracking algorithm for UAV with single-axis gimbal is proposed. Considering the non-linearity of the tracking process, fuzzy controllers are designed to control the pitch channel,

heading channel, roll channel, and the gimbal channel. Simulation results and flight tests prove the fuzzy controllers have kept the stability and reliability of the tracking system.

The detected target positions and the difference of the positions in the X-axis of image are sent to the fuzzy

controllers. The controllers then generate the command of the UAV, especially in roll channel, which can control the radius of the circle. As the target moving, the expected turn radius of the trajectory changes as well. By generating roll command from image information using fuzzy controller, the controllers can complete the task of tracking a moving target without knowing the exact mathematical relationship between deviation in the image and the expected radius. Simulation results and flight tests have proved the reliability of the tracking algorithm.

To eliminate the deviation on the Y-axis of the image, the gimbal rotates according to the output of the fuzzy controller for gimbal channel, whose inputs are the deviation in the Y-axis of image and its derivative. Results show that the algorithm is able to accomplish the task of tracking a moving target successfully. Simulation results show that the maximum angle offset of the camera's optic axis is 0.04°. In the flight test, the angle offsets can be kept in the range of 5°.

References

Asl HJ, Bolandi H (2014) Robust vision-based control of an under actuated flying robot tracking a moving target. Trans Inst Meas Control 36(3):411–424

Choi H, Kim Y (2014) UAV guidance using a monocular-vision sensor for aerial target tracking. Control Eng Pract 22:10–19

Clausi DA, Zhao YP (2003) Grey level co-occurrence integrated algorithm (GLCIA): a superior computational method to determine co-occurrence probability texture features. Comput Geosci 29(7):837–850

Dobrokhodov VN, Kaminer Member II, Jones KD, Ghabcheloo R (2006) Vision-based tracking and motion estimation for moving targets using small UAVs. Proceedings of the 2006 American Control Conference, pp 1428–1433

Dobrokhodov VN, Kaminer II, Jones KD (2008) Vision-based tracking and motion estimation for moving targets using unmanned air vehicles. J Guid Control Dyn 31(4):907–917

Frew EW, Lawrence DA, Morris S (2008) Coordinated standoff tracking of moving targets using Lyapunov guidance vector fields. J Guid Control Dyn 31(2):290–310

Fu X, Feng H, Gao X (2012) UAV mobile ground target pursuit algorithm. J Intell Robot Syst 68:359–371

Gomez-Balderas JE, Flores G, García Carrillo LR, Lozano R (2013) Tracking a ground moving target with a quadrotor using switching control. J Intell Robot Syst 70:65–78

Jabbari Asl H, Do TD (2015) Asymptotic vision-based tracking control of the quadrotor aerial vehicle. Hindawi Publishing Corporation Mathematical Problems in Engineering. pp 9–17

Jin X, Yin G, Wang J (2017) Robust fuzzy control for vehicle lateral dynamic stability via Takagi-Sugeno fuzzy approach. Am Control Conf (ACC), pp 5574–5579

Jurado F, Palacios G, Flores F, Becerra HM (2014) Vision-based trajectory tracking system for an emulated quadrotor UAV. Asian J Control 16(3):729–741

Mao J, Jain AK (1999) Artificial neural networks for feature extraction and multivariate data projection. IEEE Trans Neural Netw 6:296–317

Oh H, Kim S, Shin HS, White BA, Tsourdos A, Rabbath CA (2013) Rendezvous and standoff target tracking guidance using differential geometry. J Intell Robot Syst 69:389–405

Qadir Ashraf, Semke William, Neubert Jeremiah (2014) Vision based neuro-fuzzy controller for a two axes gimbal system with small UAV. J Intell Robot Syst 74:1029–1047

Quintero SAP, Copp DA, Hespanha JP (2015) Robust UAV coordination for target tracking using output-feedback model predictive control with moving horizon estimation. Am Control Conf. https://doi.org/10.1109/ACC.2015.7171914

Shan C, Tan T, Wei Y (2007) Real-time hand tracking using a mean shift embedded particle filter. Pattern Recognit 40(7):1958–1970

Shen J, Xin B, Cui H, Gao W (2017) Speed control of single-axis rotation INS by tracking differentiator based fuzzy PID. IEEE Trans Aerosp Electron Syst, pp 1–11

Starner T, Leibe B, Minnen D, Westyn T, Hurst A, Weeks J (2003) The perceptive workbench: computer-vision-based gesture tracking, object tracking, and 3D reconstruction for augmented desks. Mach Vis Appl 14(1):59–71

Wang X, Zhu H, Zhang D, Zhou D, Wang X (2014) Vision-based detection and tracking of a mobile ground target using a fixed-wing UAV. Int J Adv Rob Syst 11(156):1–11

Zhang Y, Xu Y, Wu Y (2017) Application of simplex method in optimal design of fuzzy controller. IEEE Autom (YAC) 6:457–461

SUN Zhao (2014) Vision-assisted Adaptive Target Tracking of Unmanned Ground Vehicles. Proceedings of the 33rd Chinese Control Conference, pp 3685–3690

Zhao L, Chen P (2015) Moving target autonomous positioning based on vision for UAV. China Satell Navig Conf (CSNC) 3:691–701

Zhu S, Wang D, Low CB (2013) Ground target tracking using UAV with input constraints. J Intell Robot Syst 69:417–429